



RESIDUAL STRESS DISTRIBUTION FOR A SINGLE PASS WELD IN PIPE

Dr. Adnan N. Jameel
Ass. Prof
University of Baghdad

Dr. Nabeel K. Abid Al-Sahib
Ass. Prof.
University of Baghdad

Dr. Osama F. Abd Al Latteef
Lecturer
University of Baghdad

ABSTRACT

Heat input due to the welding of mild steel pipe causes a temperature gradient in the parent metal. After welding and temperature cooling down, residual stresses appear around welding zone which reduces the weld strength. Residual stresses are a result of the temperature gradient and the dependency of material properties on the temperature, such as yield strength, elasticity modulus, and thermal expansion coefficient.

In this study, a typical flat joint of a single pass weld in a thin pipe was studied analytically and numerically. Analytical approach is performed by exploring a simple method to calculate the magnitude of residual stress in terms of the weld shrinkage behavior. Numerical analysis is performed by applying non-linear transient heat transfer analysis using welding parameters, such as heat generation, free or forced convection with ambient, are performed using a general purpose FE package ANSYS 8.0 in order to obtain the temperature distribution in the welded parts. A non-linear thermal-elastic-plastic stress analysis is then performed using the same package to predict the stress fields during and after welding.

الخلاصة

أن الحرارة الناتجة عن لحام الأنابيب الفولاذي يسبب تغير في درجات الحرارة للمعدن الأصل. بعد اللحام و نتيجة لانخفاض درجات الحرارة تظهر إجهاد متبقية حول منطقة اللحام مما تؤدي الى انخفاض في مقاومة المعدن. أن الإجهادات المتبقية تظهر نتيجة التغير في درجات الحرارة وتبعية خصائص المادة على درجة الحرارة، مثل مقاومة الخضوع، معامل المرونة، ومعامل التمدد الحراري. تم في هذا البحث دراسة الإجهادات الناتجة عن لحام الأنابيب الرقيقة تحليليا وعدديا. المنهج التحليلي تم فيه استخدام طريقة بسيطة لحساب مقدار الإجهاد المتبقي من ناحية سلوك إنكماش اللحام. أما المنهج العددي تم فيه استعمال تحليل نقل الحرارة العابر للاختي مع عوامل اللحام المختلفة مثل الحرارة المتولدة، و معامل الانتقال الحراري مع الجو المحيط، باستعمال برنامج التحليل العددي متعدد الأغراض ANSYS 8.0 لكي نحصل على توزيع درجة الحرارة في الأجزاء الملحومة. ثم استخدام تحليل الإجهاد البلاستيكي الحراري للاختي باستعمال نفس البرنامج لتوقع الإجهاد أثناء وبعد عملية اللحام.

KEYWORDS: Residual Stress, Weld Pipe, Thermo-elasto-plasticity.

INTRODUCTION:

In fusion welding, a weldment is locally heated by the welding heat source. Due to the non-uniform temperature distribution during the thermal cycle, incompatible strains lead to thermal stresses. These incompatible strains due to dimensional changes associated with solidification of the weld metal, metallurgical transformation, and plastic deformation, are the sources of residual stresses and distortion.

Welding-induced residual stresses and distortion can play a very important role in the reliable design of welded joints and welded structures. However, the welding process itself is a very complex phenomenon, which has not been fully understood, so that distribution and magnitude of residual stress is not readily available from the literature [Wu, 2001]. Residual stress distribution and distortion in a welded pipe are strongly affected by many parameters and by their interaction. In particular, there are structural, material, and welding factors. The structural parameters include geometry of the pipes, thickness and diameter and joint type. Among the material parameters mechanical and physical properties and type of process employed, welding procedure, current, voltage, arc travel speed, and arc efficiency. As a consequence of the non-uniform temperature distribution, parts of materials close to the weld are subject to different rates of expansion and contraction developing a three dimensional complex residual stress state.

The stresses at hoop welds in pipes have been investigated by many previous workers. The most recent researches implemented a welding simulation methodology and experimentally validated to predict residual stresses on multipass welds. The simulation involves performing thermo-elasto-plastic analysis using a consistent element activation approach in the mechanical analysis [Panagiotis, 1997].

In this paper, mathematical model and finite element simulation of the single pass welding process yielding the welding-induced residual stresses in a welded pipe is presented.

RESIDUAL STRESS DUE TO PIPE WELDING:

Residual stresses are formed by the plastic deformations during the thermal cycle of welding. Before welding, the structure is assumed to be at room temperature and free of stresses. During the weld thermal cycle, material mechanical properties change drastically, especially when material approaches melting point temperature. Therefore, due to the temperature dependence of material properties and the large deformation in fusion welding, material and geometrical non-linearity have to be taken into account. The initial expansion material due to the temperature increase is constrained by material placed away from the heat source, therefore generating compressive stress. At a temperature higher than material critical temperature, the material starts exhibiting thermal softening where heating results in decrease of flow stress. As phase change occurs deviatoric stress becomes zero and considerable plastic deformation occurs in the weld metal and the base metal regions near the weld. As temperature decreases during the cooling phase, the stress in the solidifying material increases, and becomes tensile due to the positive temperature gradient. The region placed away from the weld line, will therefore, be in compression since the resultant force and the resultant moment induced by residual stress evaluated in any plane section must satisfy translation and rotational equilibrium. The plastic strains resulting from the heating causes stress, which in turn produce internal forces that may cause buckling, bending, and rotation. These displacements are in general called distortion. The residual stress combined with distortion and

degradation of the material mechanical properties influence the buckling strength and fatigue life of welded structure [Meo, 2003].

MATHEMATICAL MODEL:

In a girth-welded pipe, shrinkage of the weld in the circumferential direction induces shearing force, Q , and bending moments, M , to the pipe as shown in Fig. (1). the angular distortion caused by butt welding also induces bending moment. Distribution of residual stresses is affected by the following [Koichi, 1980]:

- 1-The diameter and wall thickness of the pipe.
- 2-The joint design (square, butt, vee, xetc).
- 3-The welding procedure and sequence (welded on outside only, welded on both sides, outside first, or welded on both sides, inside first).
- 4-The welding parameters (current, voltage, speed, electrode diameter, type of electrode...etc).
- 5-Material properties.

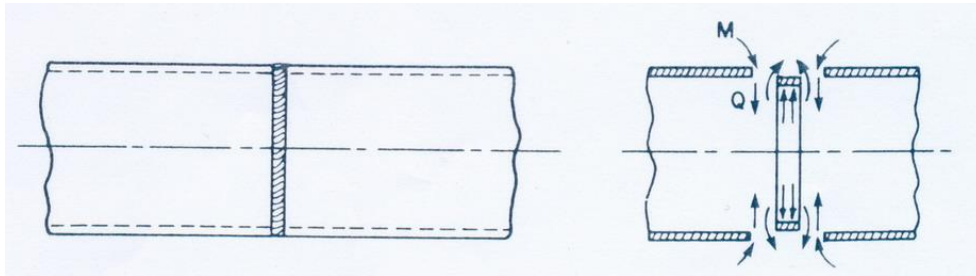


Fig. 1 Residual stresses in a welded pipe [Norman, 1984]

The tendon force locked into a weld is defined as the imaginary line load which would produce the observed shrinkage parallel to the weld, and is approximately independent of restraint. It may therefore be estimated on the basis of the assumption of infinite restraint against any hoop wise expansion of the heat material during welding. Then, the residual hoop stress at any point is a function of the maximum temperature reached, and the hoop tendon force is obtained by integrating the stress distribution.

For a surface weld bead, the maximum temperature as a function of the distance r from the weld centerline is given approximately by [Norman, 1984]:

$$T_{\max.} = \frac{2}{e\pi} \frac{\zeta q}{vr^2 \rho C_p} \quad (1)$$

Where ζ is the arc efficiency, q the weld power, v the weld travel speed, and ρC_p the volumetric specific heat.

Inside the region where the thermal strain αT_{\max} is greater than twice the yield strain σ_y/E , yield occurs in compression during heating, and then again in tension during cooling. For thermal strains between

$2\sigma_y/E$ and σ_y/E , the material yields in compression during heating, but unloads to a sub-yield tensile strain during cooling. Material whose maximum thermal strain is less than σ_y/E does not yield, and ends at zero stress for the idealized conditions of infinite hoop wise restraint.

The width of the zone containing yield magnitude tensile stresses (Fig. (2)) can be found by substituting $T_{\max.} = 2 \sigma_y/E\alpha$ in eq. (1):

$$r = \sqrt{\frac{E\alpha}{e\pi\sigma_y\rho C_p} \frac{\zeta q}{v}} \quad (2)$$

Where E modulus of elasticity, α thermal expansion coefficient, and σ_y yield strength of the pipe material.

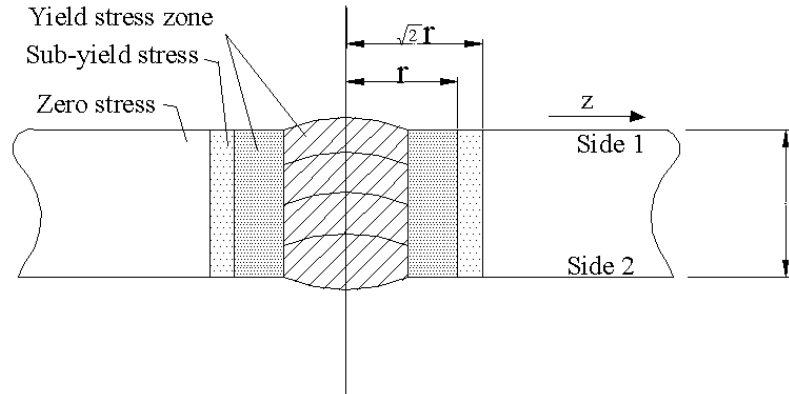


Fig. 2 Hoop tensile zone at girth weld

The total force locked into the tensile zone is given by:

$$F = A_w \sigma_{yw} + (1.17 \cdot 2t_o r - A_w) \sigma_y \quad (3)$$

Where A_w and σ_{yw} are the area and yield strength of the weld, and the factor **1.17** allows for the sub-yield tensile stresses between r and $\sqrt{2}r$.

The inward radial deflection of a circular cylindrical shell loaded symmetrically with respect to its axis [Timoshenko, 1959]:

$$y = \frac{-e^{-\beta z}}{2\beta^3 D} [\beta M_o (\cos \beta z \quad \sin \beta z) + Q_o \cos \beta z] \quad (4)$$

And hence:

$$\frac{dy}{dz} = \frac{e^{-\beta z}}{2\beta^2 D} [2\beta M_o \cos \beta z + Q_o (\cos \beta z + \sin \beta z)] \quad (5)$$

$$\frac{d^2 y}{dz^2} = \frac{-e^{-\beta z}}{2\beta D} [2\beta M_o (\cos \beta z + \sin \beta z) + 2Q_o \sin \beta z] \quad (6)$$

Where $\beta = \left[\frac{3(1-\nu^2)}{R^2 t^2} \right]^{1/4}$, $D = \frac{Et_o^3}{12(1-\nu^2)}$, and R radius of the pipe.

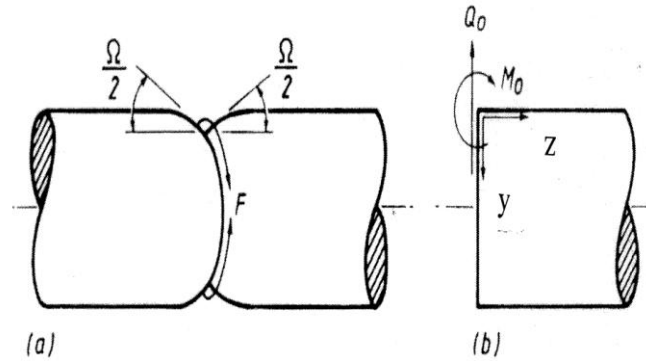


Fig. 3 (a) Shrinkage parameters Ω and F
(b) Corresponding loads at weld centerline

In order to model the deflections due to a hoop weld centered at $z=0$, the applied force Q_o and moment M_o are related to the angular distortion Ω and tendon force F which characterize the shrinkages of the weld.

The radial shear force is related to the tendon force F by considering radial equilibrium at $z=0$ [Timoshenko, 1959]:

$$Q_o = \frac{-F}{2R} \tag{7}$$

The bending moment M_o is found by setting $\frac{dy}{dz} = \frac{-\Omega_w}{2}$ at $z=0$ in eq. (5). Hence:

$$M_o = \frac{-1}{2\beta} (\beta^2 D \Omega_w + Q_o) \tag{8}$$

Substitution for Q_o and M_o in eqs. (4), (5) and (6) gives the radial deflection and its derivatives at any distance from the weld.

The axial bending stresses σ_{zb} on the inner and outer surfaces at any section inside or outside the tensile zone are a function of the curvature:

$$\sigma_{zb} = \mp \frac{Et}{2(1-\nu^2)} \frac{d^2 y}{dz^2} \tag{9}$$

FINITE ELEMENT MODELING PROCEDURES:

The FE analysis was carried out in two steps. A non-linear transient thermal analysis was conducted first to obtain the global temperature history generated during and after welding process.

A stress analysis was then developed with the temperatures obtained from the thermal analysis used as loading to the stress model.

The general purpose FE package ANSYS 8.0 was used for both thermal and stress analysis performed sequentially. The mesh used in the stress analysis was compatible to that in the thermal analysis. The material properties of the weld metal and base metal are assumed to be the same in this analysis and it is temperature dependent. The thermal and mechanical material properties are listed in table (1) & (2) respectively.

In the thermal analysis, the heat was input in four load steps as shown in figure (4). The nodal temperature solution obtained from the thermal analysis were read as loading into the stress analysis. In order to capture the residual stress induced due to the heating and cooling cycle, the temperature history needed to be read at a sufficient large number of time points, especially where the temperature gradient is large. However, the greater the number of the thermal solution steps used, the greater the computational time and the larger store space required.

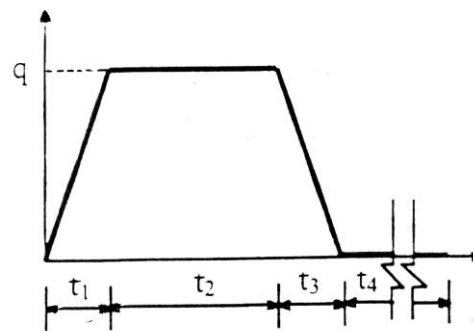


Fig. 4 Heat function input during welding [Wu, 2001]
 ($t_1=.5$ sec, $t_2=3$ sec, $t_3=.5$ sec, $t_4=396$ sec)

Table 1 Thermal material properties used in model [Brown, 1992]

NO.	T Temperature °C	K Thermal Conductivity W/m°C	Cp Specific heat J/Kg° C	h Convection heat Transfer coefficient W/m ² .C
	25	51.9	450	3
	100	51.1	486	5.4
	200	49	519	6.4
	300	46.1	557	7.0
	400	42.7	599	7.0
	500	39.4	662	7.7
	600	35.6	749	7.7
	700	31.8	816	7.7
	800	26	950	8.2
	1000	27.2	950	8.5
	1500	29.7	400	8.5
	1600	29.7	847	9.1

Table 2 Mechanical properties used in model [Brown, 1992]

NO.	T Temperature °C	σ_y Yield stress MPa	ν Poisson ratio	E Young's Modulus GPa	α Thermal Expansion $10^{-6} / ^\circ \text{C}$
	25	290	0.3	200	10
	100	260	0.31	200	11
	200	230	0.33	200	11.5
	300	200	0.35	200	12
	400	150	0.37	150	13
	500	120	0.39	110	14
	600	110	0.4	88	14
	700	9.8	0.42	20	14
	800	9.8	0.44	20	14
	1000	9.8	0.48	8	15
	1500	0.98	0.48	0.2	15
	1600	0.0098	0.48	0.00002	15

RESULTS AND DISCUSSIONS:

The sample of calculations was made on a single span ASTM214-71 mild steel pipe with (1 m) length, (25.4 mm) radius, (1.5 mm) thickness. The welded pipe was formed by joining two (0.5 m) pipes by single pass fusion arc welding. The amount of heat input was found as the product of arc efficiency, voltage, and current (Power arc welding = $f_1 f_2 VI$), Where: f_1 =heat transfer efficiency, f_2 =melting efficiency, V =voltage, and I =current. We take $f_1=0.9$, $f_2=0.6$, $V=30$ volt, $I=300$ Amp, using an electrode type E7010-G to make a straight pipe 1m length with welding on its mid span.

Fig. (5) Shows the temperature time history at a point in the center of welding. Fig. (6) Shows the temperature time history at a path along the length of the pipe at times during and after welding predicted by FE analysis. Fig. (7) Shows the nodal solution of the temperature distribution along the pipe. It was seen that max. Temperature in a center line of welding equal (1566 °C) at the moment of end welding then decreased and distributed along the pipe.

During the welding process, the temperature is locally increased to the melting point of mild steel. Moreover, in the heat affected zone of the weld, the temperature reaches high values. The mechanical properties of mild steel such as yield strength and elasticity modulus are highly depending on the temperature. After welding, the heat energy is dissipated due to convection with ambient air causing the steel to cool down and consequently gain its original yield strength. During this process of increasing and decreasing the temperature, residual stresses and plastic strains are developed.

Fig. (8) Shows the longitudinal stress time history at a path along the length of the pipe at times during and after welding predicted by FE analysis. The nodal solution of residual stress distribution

in Z-direction during and after welding along the top surface predicted by FE analysis is shown in fig. (9). It can be seen from these figures that the stress is changed from compression at the centerline of weld and tension away from the weld centerline at the end of welding ($t=3.5$ sec) to tension at the centerline of weld and compression away from the weld centerline when it cooled ($t=400$ sec), which are a good agreement between the analytical and numerical results with the published results [Wu, 2001; Erika, 2002].

The Von Mises residual stress distribution is shown in fig. (10) at time equal 400 sec. Fig. (11) Illustrates the results of residual stress distribution along the pipe due to welding. It is clear that the predicted residual stress by FE analysis is very close to the analytical analysis at the center of welding. It shows a tension peak of $\sigma_z=225$ MPa at weld line and adjacent parent metal going into compressive at about $Z=10$ mm from weld centerline and then blending into the background elastic distribution at about $Z=30$ mm from weld centerline. At position remote from the weld, the stresses didn't go to zero, but tend towards a steady value of about 10 MPa compressions. These results agree well with theoretical studies of residual stresses, at girth welds in pipes [Norman, 1984].

Fig. (12) Shows time variation of plastic strain at a centerline of welding. It is clear that the plastic strain increases rapidly during welding and then still constant during cooling.

The average values of thermal properties over the applied temperature distribution were used to study the effect of temperature dependent material properties on the final residual stress results. The residual stress obtained from the FE analysis using constant thermal properties show a significant difference from the obtained using temperature dependent thermal and mechanical properties as shown in fig. (13), especially in the heat affected zone due to the fact that the yield strength variation at higher temperature has less effect. This suggested that care must be taken to identify correctly the temperature-dependent yield strength of material which is often not easily determined.

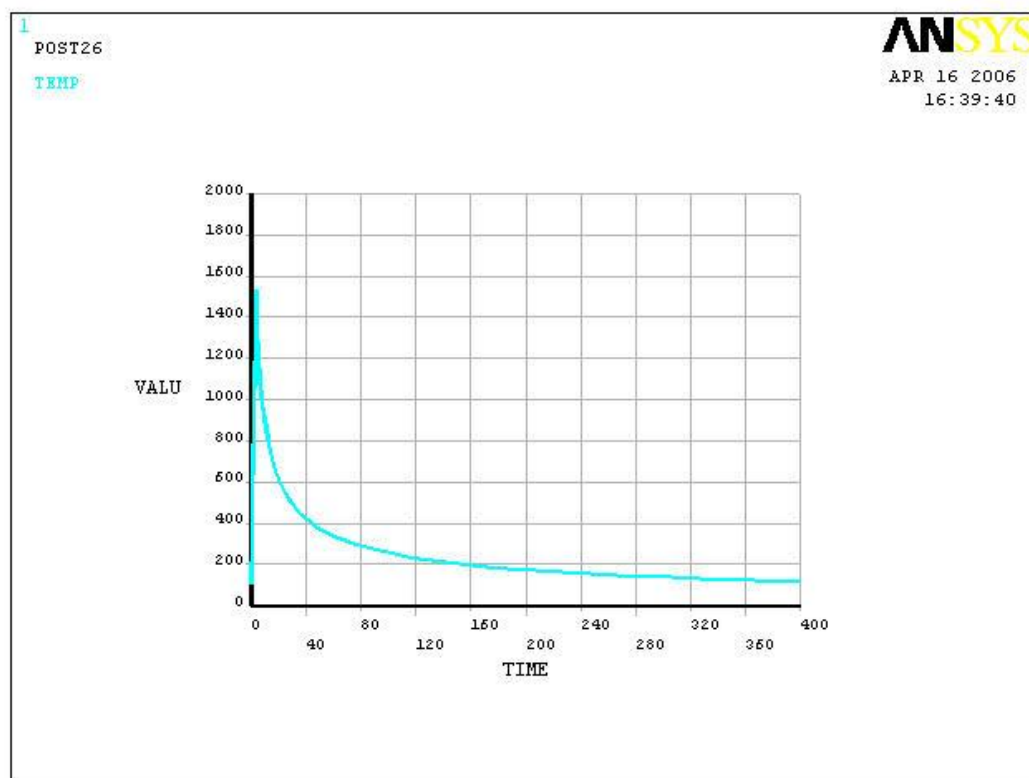


Fig. 5 Temperature time history at a point in the center of welding

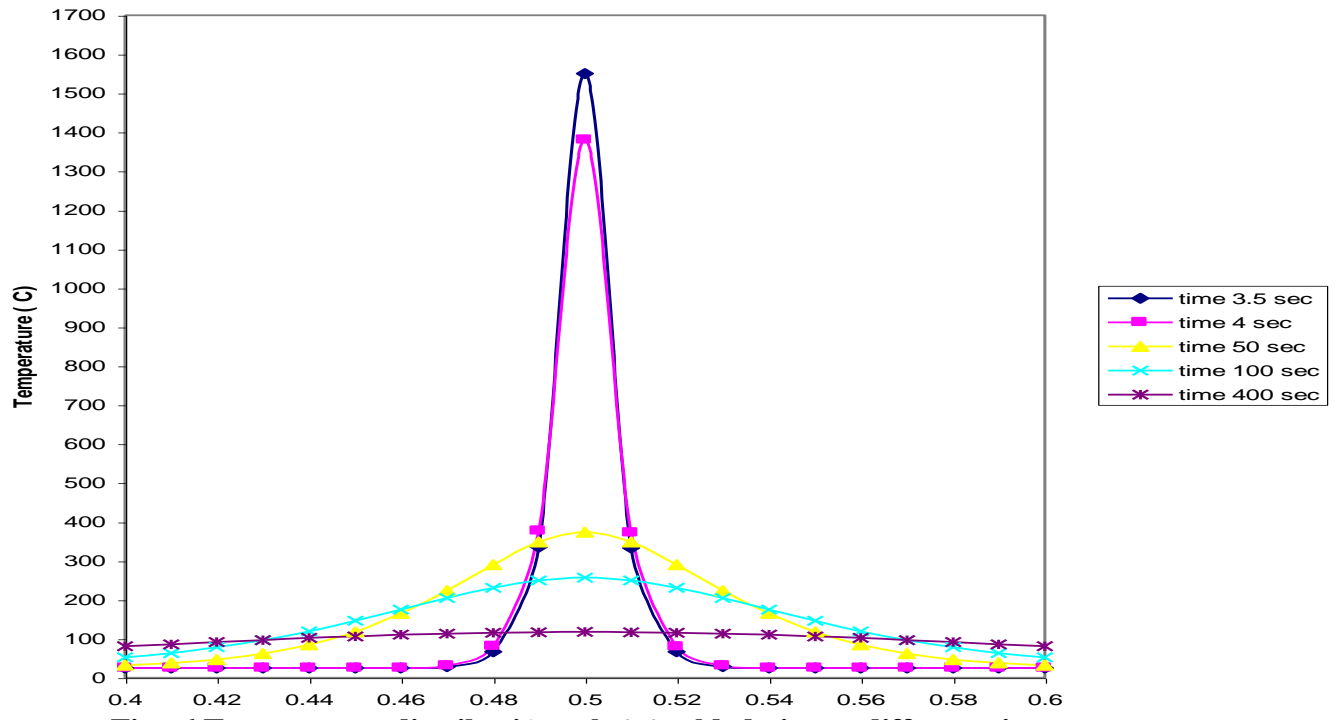


Fig. 6 Temperature distributions along welded pipe at different times

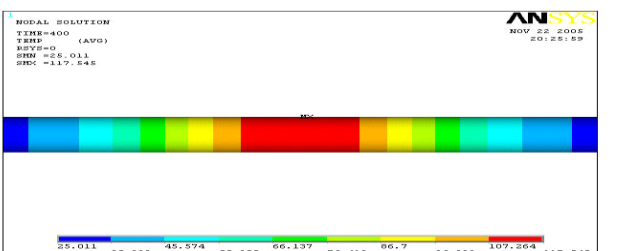
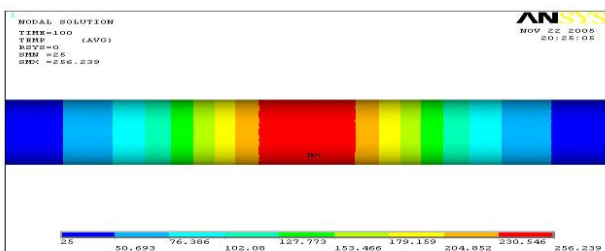
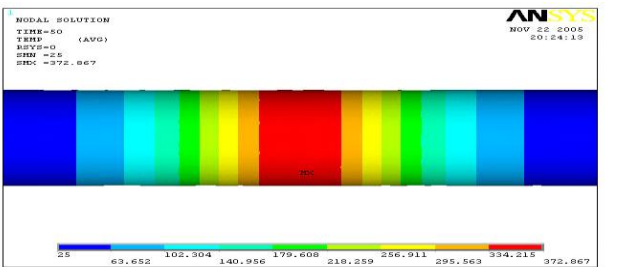
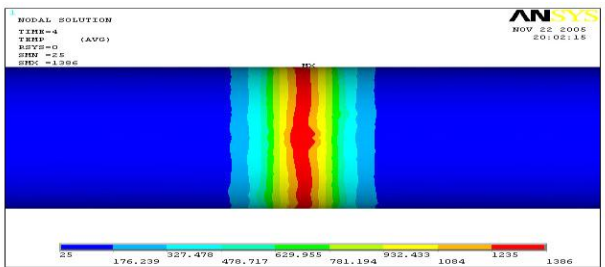
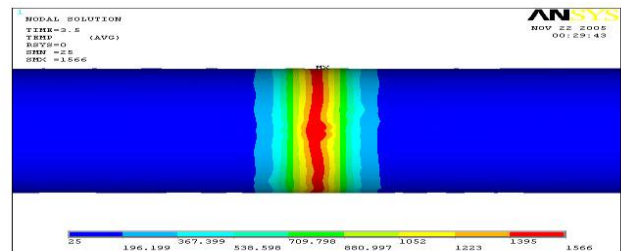
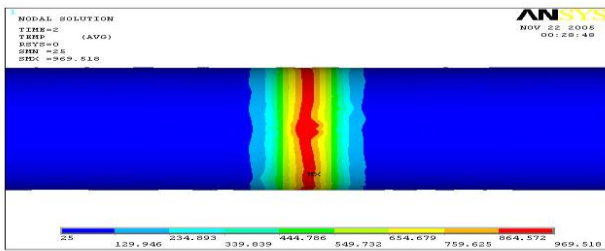


Fig. 7 Temperature distribution during and after welding

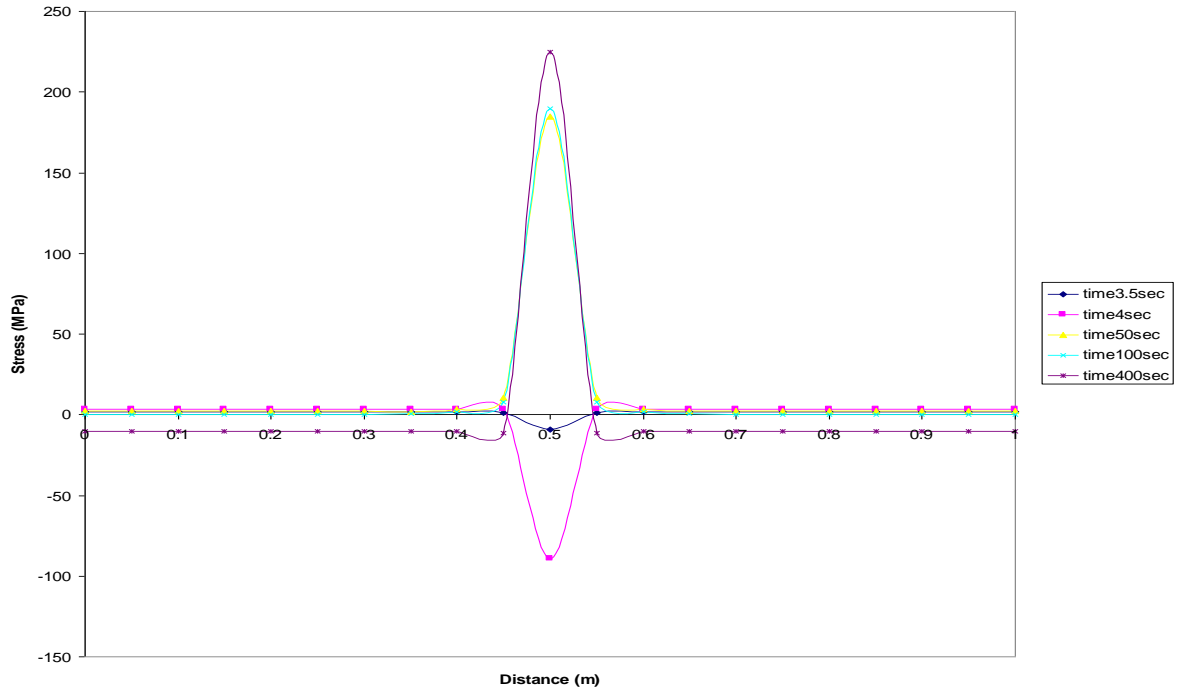


Fig. 8 Residual stress distributions along welded pipe at different times

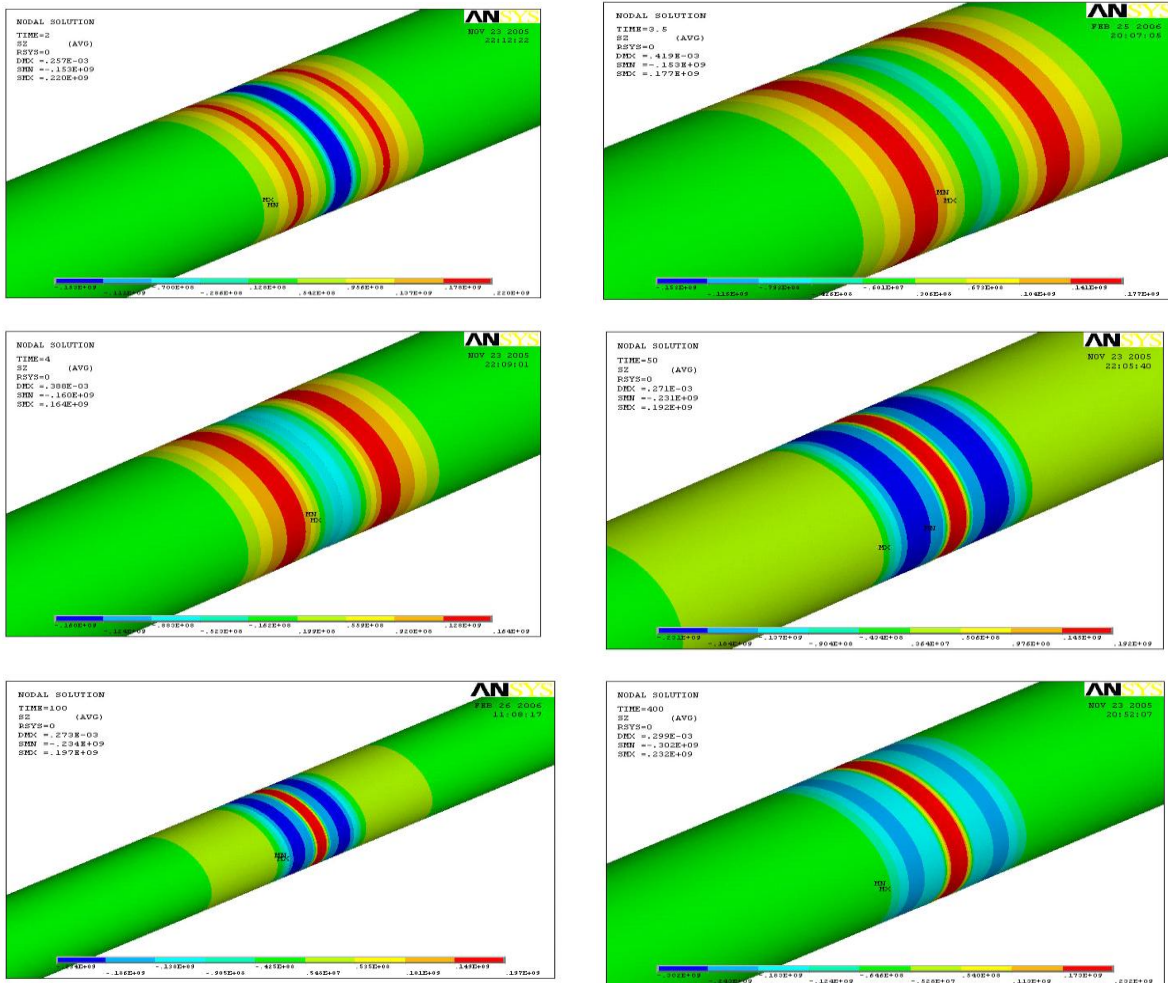


Fig. 9 Residual stress distribution along welded pipe during and after welding

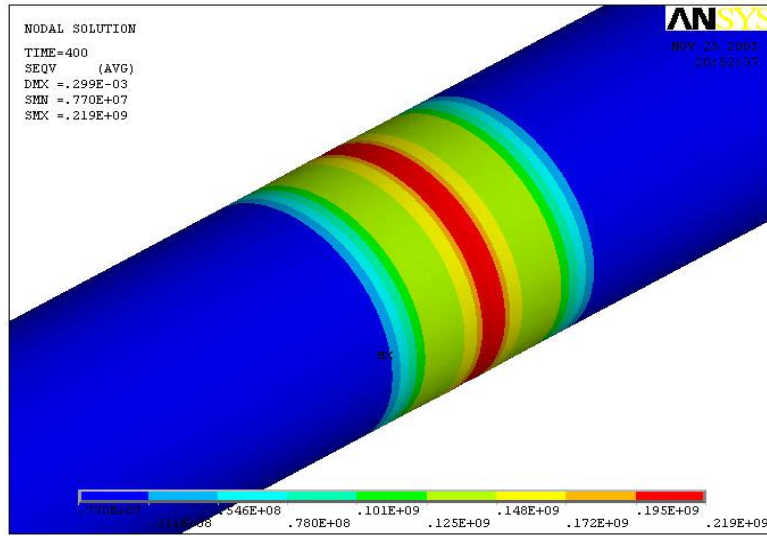


Fig. 10 Von Mises residual stress distribution in a welded pipe

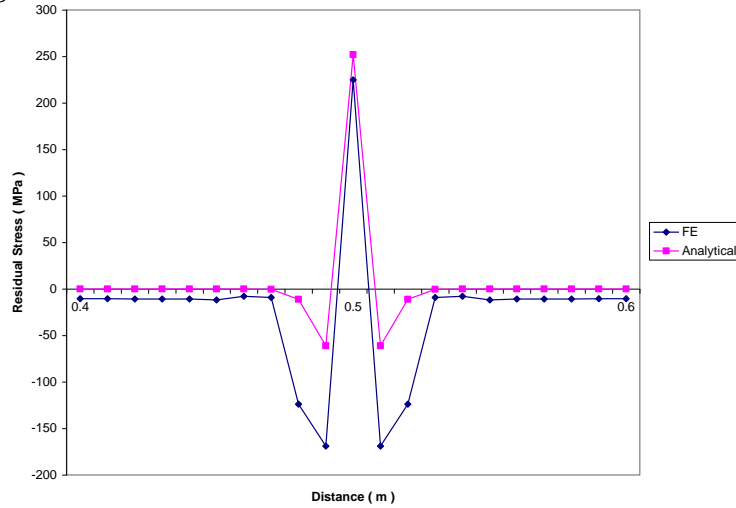


Fig. 11 Residual stress distribution along welded pipe

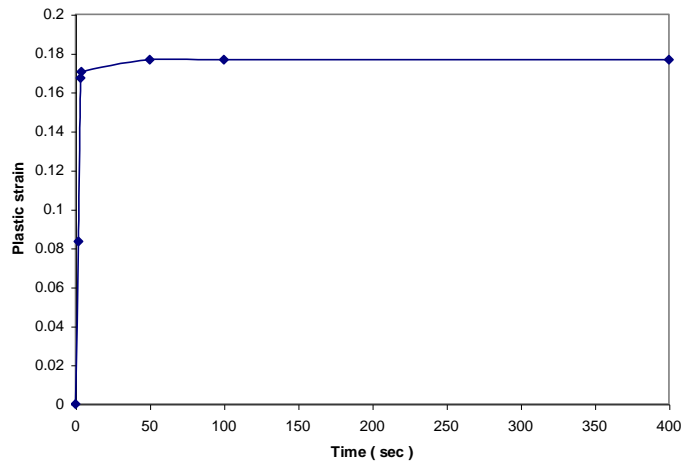


Fig. 12 Plastic strain in a centerline of weld

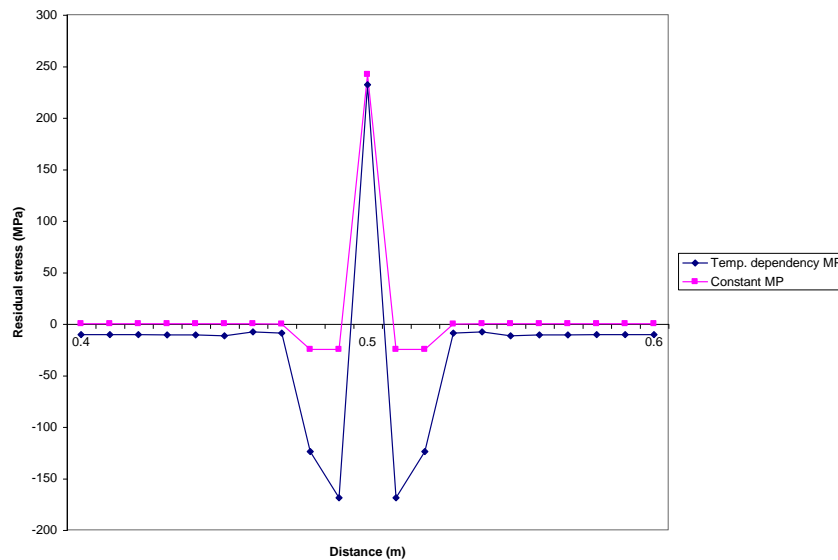


Fig. 13 Effect of temperature dependency material properties on the residual stress along a weld pipe

CONCLUSIONS:

Analytical and finite element analysis are used to determine the residual stresses resulting from the single pass welding of mild steel pipe of 25.4 mm radius, 1.5 mm thickness. Following the main summarized conclusions raised by this paper:

- 1- Welding of a pipe induced residual stresses. It has been seen that these stresses changed from compression at the centerline of welding and tension away from the weld centerline at the end of welding to tension at the centerline of weld and compression away from the weld centerline when it cooled.
- 2- The residual stress obtained by using constant thermal and mechanical properties show significant difference from that obtained using temperature dependent thermal and mechanical properties especially in the heat affected zone.

REFERENCES:

- Brown S. and Song H., "Finite element simulation of welding of large structures", Vol.114, November 1992.
- Erika Hedblom, " Multipass welding of nuclear components-computations ", Lulea University of Technology, Department of Applied Physics and Mechanical Engineering, Division of Computer Aided Design, 2002.
- Koichi Masubuchi, " Analysis of welded structures (residual stresses, distortion, and their consequences), 1980.
- Meo M. and Vignjevic R., "Welding simulation using FEA ", College of Aeronautics, Cranfield University, Bedford, UK, MK430AL,2003.



- Norman Eaton, "Welding in energy-related projects ", Welding Institute of Canada, 1984.
- Panagiotis Michaleris, "Residual stress distributions for multi-pass welds in pressure vessel and piping components ", Edison Welding Institute, Columbus, 1997.
- Timoshenko S. and Woinowsky-Krieger S., "Theory of Plates and Shell", second edition, McGraw-Hill, 1959.
- Wu A., Syngellakis S., and Mellor B.G., "Finite Element Analysis of Residual Stresses in a Butt Weld", University of Southampton, High field, U.K, 2001.

NOMENCLATURE

<i>Symbols</i>		<i>Units</i>
A_w	Area of the weld	m^2
C_p	Specific heat of pipe material	$J/Kg^{\circ}C$
E	Modulus of elasticity	N/m^2
F	Tendon force	N/m
M_o	Bending moments	Nm
Q_o	Shear force	N
q	Weld power	watt
R	Radius of the pipe	mm
T_{max}	Maximum temperature at the weld	$^{\circ}C$
t_o	Thickness of the pipe	mm
v	Weld travel speed	m/sec
ζ	Arc weld efficiency	
ρ	Density of pipe material	Kg/m^3
α	Thermal expansion	$^{\circ}C$
σ_y	Yield stress of a pipe metal	N/m^2
σ_{yw}	Yield stress of the weld	N/m^2
σ_{zb}	Axial bending stress	N/m^2
Ω_w	Angular distortion	